PERFORMANCE INVESTIGATION OF CAMERAS USING HDR SENSORS FOR DAYLIGHT GLARE EVALUATIONS

Kim, D.H.[1], Quek, G.[1,2], Wienold, J.[1]

[1]LIPID, École Polytechnique Fédérale de Lausanne (EPFL), Lausanne, Switzerland

[2]Architecture and Sustainable Design, Singapore University of Technology and Design (SUTD), Singapore, Singapore

donghyun.kim@epfl.ch

Abstract

This study presents a novel framework for evaluating the luminance measurement capabilities of High Dynamic Range (HDR) sensor cameras in indoor glare conditions. Results indicate that the practical usage range of the CSEM VIP camera is significantly lower than specified, but it provides reliable measurements within its range (around 10% difference up to 30 kcd/m^2 compared to ILMDs). The TRI054S camera demonstrates reliable measurements under much higher illumination with an error of less than 10%. However, in lower luminance areas when intense glare is present, it produces noise, making analysis challenging compared to the performance of ILMDs. This limitation may be overcome by merging images taken with and without an ND filter. Overall, HDR sensor cameras show potential for real-time monitoring of rapidly changing luminous environments and could provide personalized glare measurements when used as wearable devices.

Keywords: Luminance map, HDRI, Glare, ILMD, Calibration

1 Introduction

High-dynamic-range (HDR) imaging technology, which enables spatial luminance distribution measurements, has become a useful tool for glare evaluations, both for indoor and outdoor scenarios. Conventional methods (Ward, 1998; Ward, 2011; Mantiuk *et al.* 2007) rely on capturing and merging low dynamic range (LDR) images at varying exposure times using DSLR cameras with RGB sensors or scientific-grade manufacturer-calibrated imaging luminance measurement devices (ILMDs). The former method, often referred to as the 'self-calibration method' or 'multiple exposure method', may introduce uncertainties due to variations in HDR algorithms, motion artifacts, and the potential for pixel saturation.

Recently, the development of HDR image sensors capable of capturing wide dynamic range images in a single or continuous exposure has opened new possibilities. These sensors, widely used in the automotive industry, have the potential to minimize the uncertainty associated with the multiple exposure method. However, while few studies have explored the signal characteristics of these sensors in lab settings (Ledig *et al.,* 2019), their application in real-world glare studies, especially in comparison with ILMDs, remains largely unexplored. Such scenarios may include extreme contrasts that challenges both sensors and algorithms. Moreover, there is no established method to compare the luminance measurement performance of these different camera hardware.

Addressing these gaps. This study has three following objectives:

i) To propose a method for comparing the performance of HDR measurement in glare evaluation.

ii) To investigate the pixel-to-luminance signal characteristics of cameras equipped with two different HDR sensors; one sensor with a constant exposure time and different sensitivities and another sensor with logarithmic compression pixels.

iii) To compare the performance of these HDR sensors in measuring luminance and illuminance of glare sources and background areas against measurement results from the ILMD.

2 Methodology

2.1 Cameras and Light equipment

This study employed several types of lighting equipment and two state-of-the-art HDR sensor cameras. As reference one manufacturer calibrated ILMD (TechnoTeam LMK98-4 color camera) as well as a spot luminance meter (Konica Minolta LS-110) are used. Table 1 outlines the specifications of the different camera types used. The CSEM VIP and LUCID cameras were equipped with fisheye lenses, and corrections such as adjusting the projection, distortion functions, and vignetting curves were applied following a series of measurements in a darkroom lab environment as recommended by Pierson *et al.* (2021).

The tested cameras captured images in the RAW format. The processing of these images into final HDR images was carried out using a custom Python script, incorporating methods from Thomas *et al.* (2022) and Mantiuk *et al.* (2007) for colour demosaicing and conversion from OpenEXR to Radiance HDR format.

Table 1 – Characteristics of the camera hardware used in this study

Camera	Accessories	Image sensor	Integration time	Original output	Processed HDR image
CSEM VIP camera	A fisheye lens (SVL-01020B5M, 185°) and a photopic filter (Omega 558BP100)	Monochrome (320×240)	Single (up to several 10ms)	10-bit RAW	237×237(180°), Radiance HDR format
LUCID TRI054S camera	A fisheye lens (FE185CO57HA-1, 185°) and an ND2 filter	RGB CMOS (2860×1860)	Single (up to 0.15s)	24-bit Bayer RGGB RAW	1954×1860 (180°(h),171°(v)), Radiance HDR format
TechnoTeam LMK98-4 color camera	A fisheye lens (182°) and an ND2 or ND3 filter	Monochrome CCD (2448×2050)	Multiple exposure, (up to 15s)	Processed HDR image (.pf format)	1996×1996(180°), Radiance HDR format

Two light sources were mainly employed in this study. The first was a laser-based LED light source, demonstrated by Krasnoshchoka (2019). This light source peaks at 450 nm and is used in combination with two diffusing films (OptSaver L-52 and 3M ENVISION 50). In this setup a homogenous spot of with diameter of 30 mm can be generated reaching up to 600 kcd/m². Without the diffusing films, the maximum luminance of this light source could exceed 100 Mcd/m², making it a suitable artificial glare source for this study. The second type of light source, a halogen lamp, was used as broad-band light source to illuminate a variety of surfaces, including a white diffusing surface and a colour checker. Figure 1 shows the photographs of these two light sources and their respective spectral power distributions.

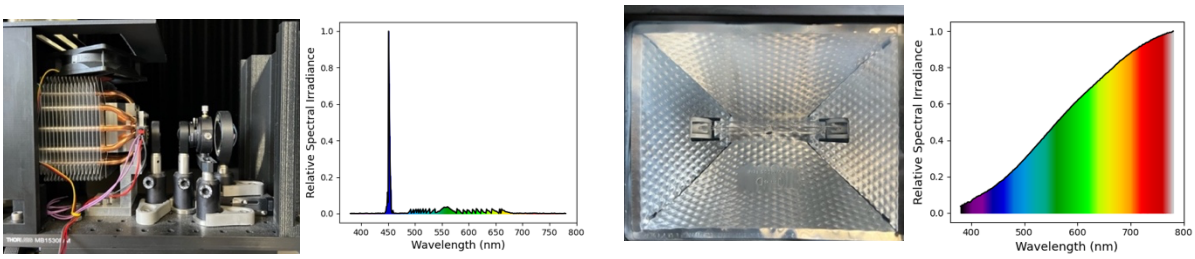

Figure 1 – Laser-based LED light source (left) and halogen lamp (right)

2.2 Calibration of HDR Sensor Cameras

The CSEM VIP camera technology was introduced to glare evaluation by Motamed (2017) and has a fixed internal integration time, requires an absolute calibration before it can be applied in glare measurements. This is necessary because its output signal (10-bit, 0 – 1023) needs to correspond to absolute luminance values in the real world. This study examined the VIP camera's signal output and its corresponding absolute luminance value across a range of 3.25 cd/m² to over 100 Mcd/m² through 290 comparisons (see Figure 2).

The luminance range from 3.25 cd/m² to 235 cd/m² was evaluated using grayscale patches on a color checker under various electric lighting conditions. The 1 kcd/m² to 1Mcd/m² range was assessed by manipulating the light incident on a diffusing acrylic panel—this involved adjusting the distance of a laser-based LED from 100mm to 500mm and using different diffusing films in a darkroom environment. A photometric calibrated spot luminance meter was used as the reference for absolute luminance values. For luminance values above 1 Mcd/m², natural sunlight was used. The luminance of the visible sundisk was evaluated under various transmittance-levels of colour-neutral panels, with the LMK98-4 color camera being used for reference measurements. Based on the above measurements, a pixel-to-luminance characteristic of the VIP camera is derived and is shown in Figure 2.

A logarithmic behavior of the luminance-to-pixel-value curve is observed within a range of 1 kcd/m² to 100 kcd/m². Above 1 Mcd/m2, however, a negative slope of the signal characteristic is observed – a behaviour also reported by Ledig *et al.* (2019) – indicating that the output pixel value decreases as the luminance increases. Consequently, the reverse function (pixel-to-luminance) is no longer unique above a level of 30 kcd/m^2, which limits the practical application of the CSEM VIP camera. To determine the best-fitting logarithmic response curve for the pixel-to-luminance dataset, the "LINEST" function in Excel was employed to estimate the parameter a, b and c in the equation $y = e^{(ax+b)} - c$. The resulting curve, shown in Figure 2, represents the best-fitting logarithmic response.

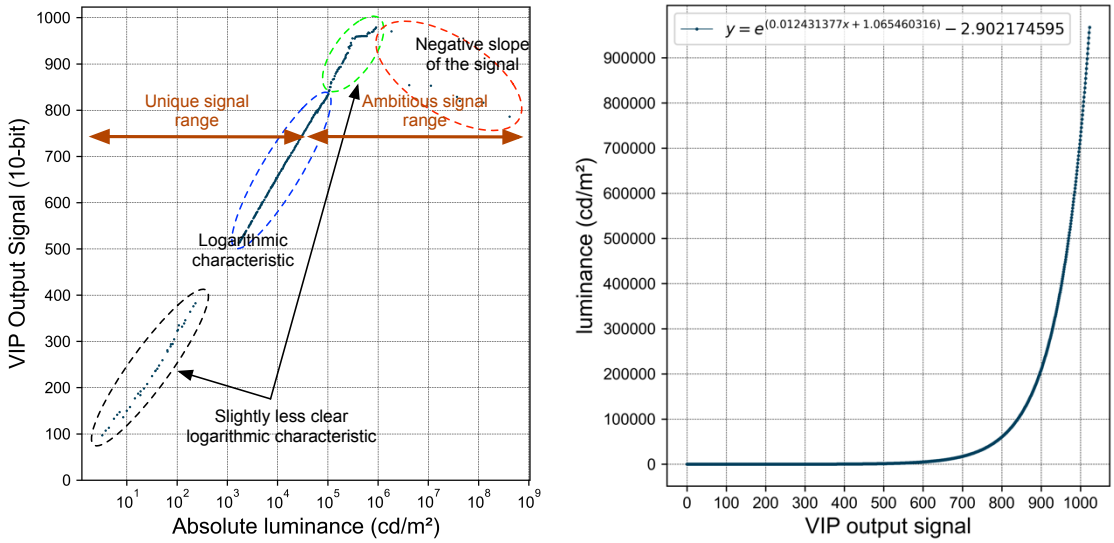

Figure 2 – Pixel signal of the VIP camera versus absolute luminance levels referenced by a photometric spot luminance meter (left) and the equation derived from the measurements that are used in the final calibration of the camera (right)

For the TRI054S camera, it allows to users to control its integration time (up to 0.15s). Given that the camera shows a linear characteristic in pixel-to-luminance relations (Lida *et al.,* 2018), a linear calibration factor is sufficient to convert pixel values into absolute luminance values. This study derived three calibration factors (CFs) under three different light sources. Under a fluorescent floor lamp condition (3,950K) at an integration time of 0.1s, a CF of 0.0086 was derived. Under a halogen lamp (2950K) at the same integration time, a CF of 0.00558 was calculated. Lastly, under clear daylight conditions, a CF of 0.0051 was observed. The CF is linearly proportional to the camera setting's integration times, meaning that if a scaling factor of 0.00558 is applied for 0.1s, a factor of 0.00058 is applied for 0.01s exposure values.

2.3 Test Environment Setup

The first setup (hereafter referred to as Scenario A) aimed to compare the performance of luminance measurement of a uniform, less intense glare source (up to 30 kcd/m^2). This setup was specifically designed to test performance of the VIP camera, which as mentioned earlier, has a limited practical usage due to its ambiguous signal range. Ten conditions (A1 to A10) were configured in Scenario A, varying the average luminance of the glare source, located at the center of the image, as shown in Figure 3a.

The second setup (hereafter referred to as Scenario B) was designed to investigate the performance in measuring a less uniform, yet more intense glare source. This condition aimed to replicate a large contrast found in real-world scenes, such as the sun seen through a roller shade fabric. Seven conditions (B1 to B7) were configured in Scenario B (see Figure 3b). In each of these conditions, the luminance value on grayscale patches (from the color checker) remained constant, while only the laser-based LED light source was modified. This was achieved by placing the laser-LED light source (glare source) ahead of the color checker and maintaining the intensity of the fluorescent lamp illuminating the color checker throughout the test conditions. Therefore, the objective of Scenario B was to verify whether the camera could accurately measure the glare source while correctly measuring the luminance of the grayscale patches. It is important to note that the round lamp and the fluorescent lamp in this scenario are not treated as a glare source, they are included to match more the real-life scenario to have some mid-range luminance values in the scene.

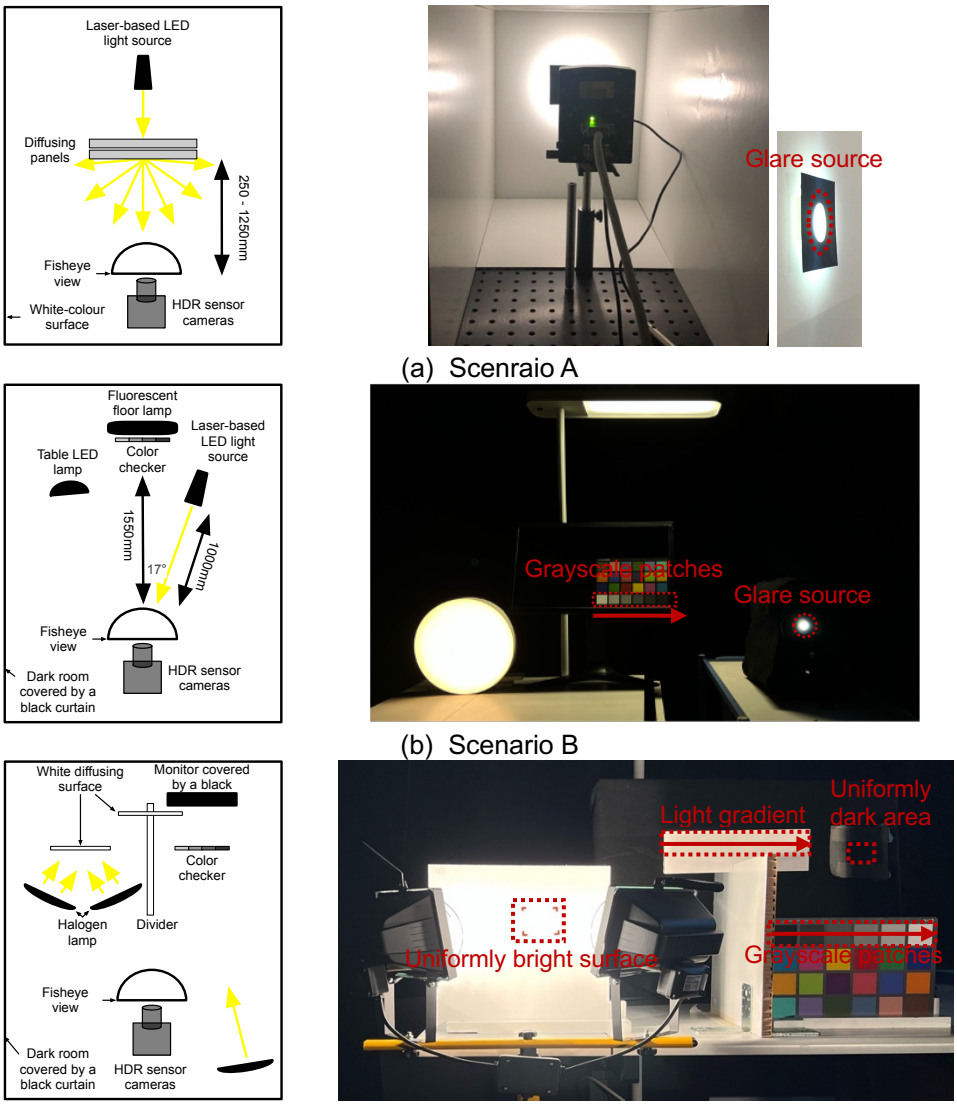

Figure 3 – Three different setups for the Scenario A,B, and C. The left side shows simplified sketches of each setup, and the right side presents photographs taken from the corresponding setups. Areas of interest in each scenario are denoted by red dotted boxes and red solid arrowed lines indicate the axis direction used to analyse the data

The third setup (hereafter referred to as Scenario C) aimed to replicate the typical range of luminance values commonly observed as background in daylight glare situations (e.g., sky, clouds, and indoor walls). As shown in Figure 3c, two halogen lamps illuminated the white surface, creating a uniformly bright area. The color checker was lit by a halogen lamp mounted further behind the measurement point.

Additionally, a horizontally cut piece of white surface displayed a light gradient from bright to dark. These elements are intended to be representative of those typically found in indoor glare situations as background luminance.

2.4 Ground-Truth Luminance, Illuminance Measurements

Table 2 to Table 4 provide the ground-truth (GT) luminance and illuminance values of the glare source used for the three test environments (Scenario A, B and C). These values were measured using either a photometric spot luminance meter, a calibrated illuminance meter (LMT Pocket Lux2) or the LMK98-4 color camera.

For Scenario A, GT luminance values were referenced by a photometric spot luminance meter (average of 1/3° opening angle) and the LMK98-4 color camera (average of 2° opening angle). For Scenario B, directly measuring the GT luminance value of the glare source was challenging due to its small size, high intensity, and non-uniform illumination. This was particularly the case when using an ILMD with a fisheye lens. Issues such as pixel overflow and lens flare occurred. Therefore, the ground-truth average luminance of the glare source was calculated indirectly. This method, referred to as 'illuminance-driven source luminance' in this study employed the known size of the glare source (a 25mm circle, equivalent to a 1.5° angular diameter from a fisheye lens), the location of the glare source (1,000mm from the camera), and the angular distance (17°). The glare source illuminance was first determined using the illuminance meter both with and without the glare source and then calculated by subtracting the latter from the former. It's important to note that the illuminance sensor has a maximum uncertainty of 0.8%, which was considered into the estimation of the illuminance-driven luminance under different Scenario B conditions. In Scenario C, a spot luminance meter was used for reference luminance values, except for the gradient surface, where the LMK camera was used for the reference.

Table 2 – Ground-truth luminance of glare source under Scenario A

Scenario A	Average luminance (cd/m^2) of glare source	
Setting No.	Spot meter	LMK camera
A1	930	924
A2	1,515	1,455
A3	1,988	1,942
A4	4,104	4,042
A5	7,030	6,961
A6	9,603	10,012
A7	13,880	14,053
A8	20,353	20,070
A9	25,300	25,690
A10	29,790	30,084

Table 3 – Illuminance and source-driven average luminance of the glare source under Scenario B

Scenario B	Glare source illuminance (lx)		Illuminance-driven luminance (cd/m^2) of the glare source	
Setting No.	Min	Max	Min	Max
B1	54.8	61.2	107,563	120,747
B2	81.6	88.4	160,166	174,413
B3	180.8	189.2	354,879	373,292
B4	380.2	391.8	746,267	773,022
B5	969.4	990.6	1902,,766	1,954,457
B6	2011	2049	3,947,249	4,042,683
B7	6277	6383	1,232,0678	12,593,680

Table 4 – Ground-truth luminance values under Scenario C

Areas of interest in Scenario C	Spot luminance (cd/m^2)
Uniformly bright surface	11,463
Gray scale patches (left to right)	5.5, 12.1, 25.7, 48.5, 75.7, 105
Surface with gradient shades	See Figure 7b
Uniformly dark surface	0.21

2.5 Luminance and illuminance calculation from calibrated HDR images

In this study, the performance comparison of luminance measurement across different cameras relied on either solid angle data or angular diameter instead of pixel count due to the camera's varying resolution.

In Scenario A, where the average luminance of the glare source was the primary focus, the source's center was first identified and the average luminance within a 2º opening angle was derived using the *Evalglare* software program.In Scenario B, a similar approach as in Scenario A, was used but with a varying opening of 1.5º to 5º to derive the average luminance values of the glare source and source illuminance.

To compare performance of luminance measurements on non-uniformly bright surface area, First, the areas of the interests were cropped (as shown in red-dotted boxes in Figure 3). Per-pixel solid angle data, and corresponding luminance data were extracted using *Radiance*'s 'pcomb' and 'pvalue' commands respectively. The focus was to analyse luminance changes across the surface in the left-to-right axis direction, indicated by the red solid arrowed lines in Figure 3. Averaging values in each column, we obtained a sequence of accumulated solid angle data and corresponding luminance values.

In Scene C, the method to compare uniformly bright and dark surfaces was similar to that of Scenario B. The only distinction was in the data presentation; instead of averaging across the vertical plane, the luminance values were sorted in a descending order from highest to lowest.

By plotting luminance values on the y-axis against the accumulated solid angle on the x-axis for each type of HDR sensor camera (as shown in Figure 6 and Figure 7), we directly compared their effectiveness in measuring luminance values on different surfaces, considering their differences in camera resolutions.

3 Results

3.1 Luminance Measurement Performance of VIP Camera- scene A

The VIP camera's luminance measurement performance (scene A) is outlined in this section. The camera was placed at three different measurement distances (250mm, 750mm, 1250mm) from the light incident, which was a 30mm circle. Figure 4 presents the luminance values measured by both the VIP and the LMK cameras (averaged over a 2º opening angle), along with the values measured by a spot luminance meter.

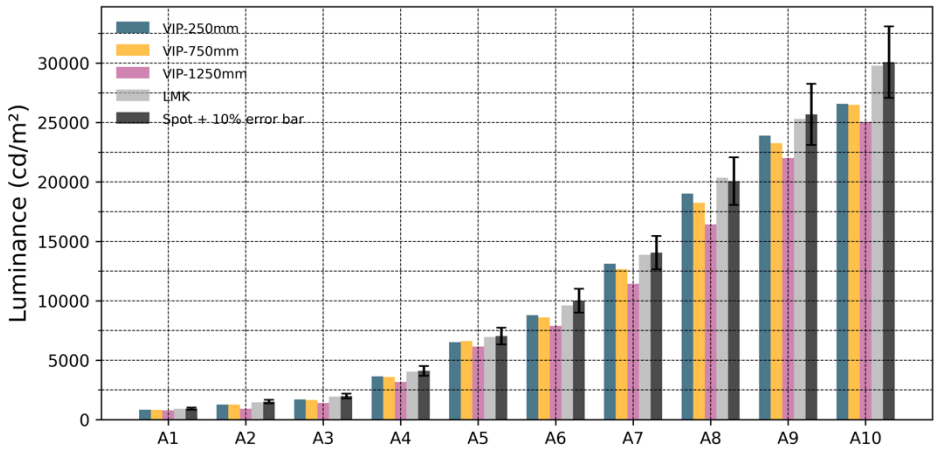

Figure 4 – Plots of illuminance-opening angle showing the comparison results in scene A

The measurements from the VIP camera generally showed a 10% difference in comparison with the ground-truth (GT) values from the LMK camera when the measurement distance was 250mm. As the measurement distance increased, the performance of the VIP camera typically dropped, with the differences increasing to 40%, but the overall trend was between 20-25%. These results indicate that to accurately measure the luminance of the glare source (up to 30 kcd/m^2) a minimum of 9 pixels is needed. When fewer than 3 pixels (measurement distance of 1,250mm), the performance of the camera significantly decreased. This outcome is expected to be a general problematic of the resolution needed to properly characterize a glare source rather than specific to the VIP camera. However, due to the low sensor-resolution of the VIP camera it is very likely to happen when a fish-eye lens is applied.

3.2 Performance Investigation with Non-Uniform Intense Glare Source – scene B

This section presents the performance evaluation results under scene B. Measurements from the VIP camera were included only for conditions B1 to B4. For conditions B5 to B7, the measurements significantly differed to the GT values mainly because of the negative signal slope characteristic under intense lighting conditions, as explained in Figure 2.

Figure 5 shows a comparison of the camera-driven illuminance values with the ground-truth source illuminance values. The camera-driven illuminance values were calculated with a varying opening angle from 1.5° to 5°, where the actual glare source size was 1.5° angular diameter. As expected, the LMK camera provided accurate results under settings B1 to B5, with less than a 5% difference to GT source illuminance values (at B6, less than 10% difference). However, at B7, we measured a significant difference between LMK-driven illuminance value and the GT source illuminance. This was caused by pixel overflow in the LMK image, despite the use of an ND3 filter.

The TRI054S camera also demonstrated relatively high level of accuracy in measuring source illuminance, less than a 5% difference under B5 to B7 settings (an ND2 filter was inserted) and less than a 10% difference under B1 to B4 settings). The VIP camera also showed accurate results under B1 and B2 setting, with a difference of less than 5%. However, its performance decreased under B3 and B4 conditions, with around 25% difference. Again, a minimum of 9 pixels, equivalent to a 3° opening angle here was required for VIP camera to perform well.

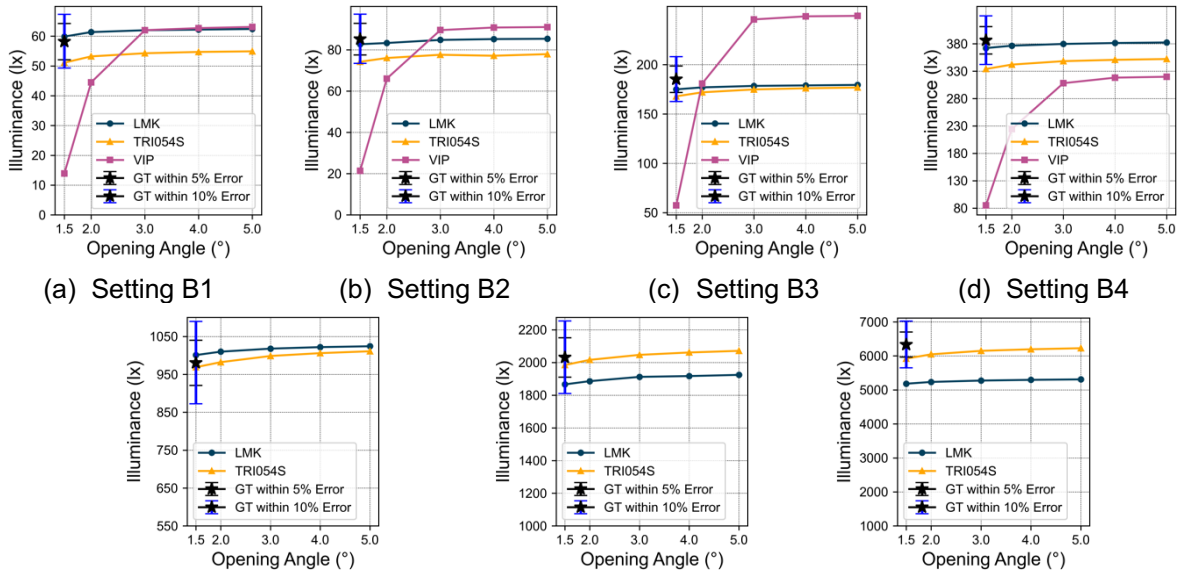

Figure 5 – Plots of camera-driven illuminance and GT source illuminance under Scene B

Incorporating these results with measurements of grayscale patches from the color checker (Figure 6) provides a more comprehensive understanding of the cameras' performance under challenging conditions. For instance, conditions B5 to B7 were particularly demanding, as the cameras needed to correctly measure grayscale patches in the presence of an intense, non-uniform glare source. Figure 6b and 6c reveal that the LMK camera closely approximated the GT values for the first three grayscale patches (white, N8 and N6.5), even under B5 and B6 settings. The increased error observed for the right three grayscale patches (N5, N3.5 and black) can be explained by a lens flare effect. In contrast, the TRI054S camera resulted in considerably noisy luminance values for the grayscale patches under B5 and B6 settings, and measurements under B7 appeared entirely noisy. Yet, under conditions B1 to B4, both the LMK and TRI054S cameras accurately measured the grayscale patches, as can be seen in Figure 6a.

Given the VIP camera's limited resolution, its performance evaluation for grayscale patch measurements seems inappropriate. Finally, Table 5 provides the calculated average luminance of the glare source from both the LMK and TRI054S cameras. These values can be directly compared to the source-driven average luminance of the glare source, which was specified in Table 3.

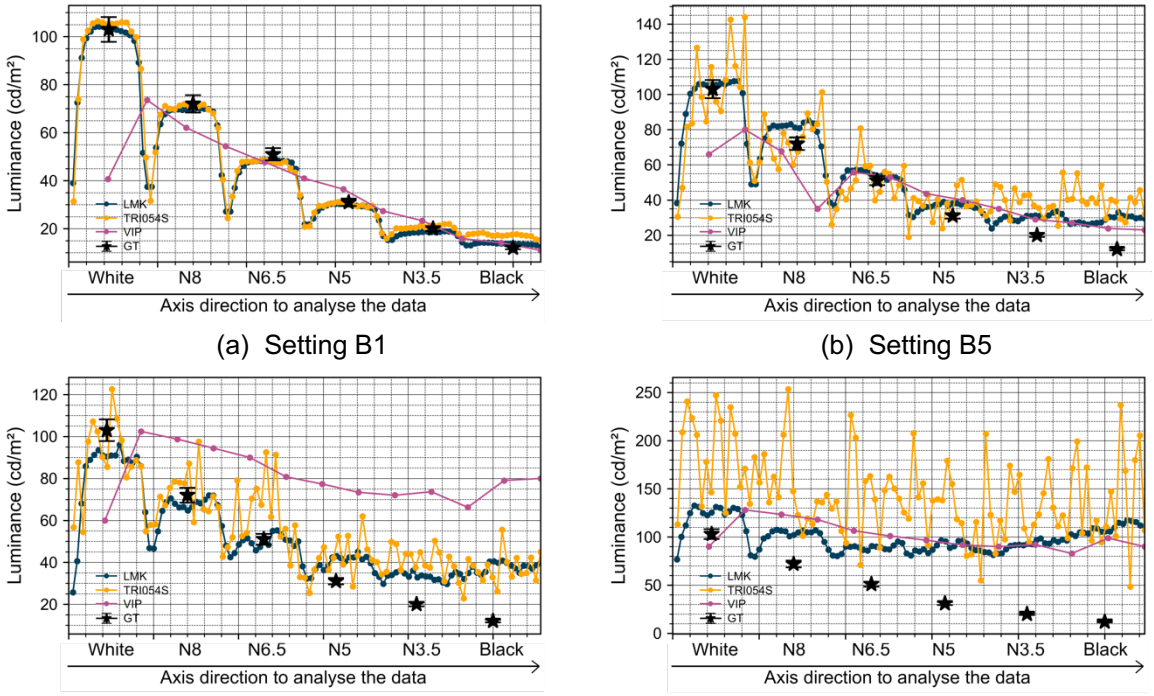

Figure 6 – Plots of luminance values on the grayscale patches under the Scene B

Table 5 – Average luminance measured from HDR camera and illuminance-driven source luminance

	Average luminance from (1.5° opening angle, LMK98-4)	Average luminance (1.5° opening angle, TRI054S)
B1	128,181	99,610
B2	163,885	143,684
B3	345,679	325,167
B4	729,416	646,086
B5	1,949,599	1,853,970
B6	3,702,532	3,835,480
B7	10,292,705*	11,712,101

*Pixel overflow occurred in the LMK image under B8 setting

3.3 Performance investigation with the illuminated surfaces – scene C

This section explains the results from Scenario C, which consisted of four comparison spots: a uniformly bright surface, a surface with gradient shades, grayscale patches from the color checker and a uniformly dark surface. The ground-truth luminance values for these areas are shown in Table 4. Figure 7 illustrates the performance of the different HDR cameras on those four spots.

More specifically, Figure 7a shows all the pixel values in the defined area (uniformly bright surface) and sorted in descending order and scaled by solid angle. Both the LMK and TRI054S camera demonstrate high uniformity up to a solid angle size of 1.5e-3 sr. Beyond this point, there is a sharp drop in the luminance values, likely due to the red marks on the surface corner. Average luminance values for the uniform bright surface were computed for the different cameras at a solid angle of 1.5e-3 sr. For the surface with gradient shades, both LMK and TRI054S cameras produced nearly identical results, with

the VIP camera also closely aligning with these outputs (less than 10% difference) as shown in In Figure 7b.

Regarding the grayscale patches in scene C, both the TRI054S and VIP cameras measured luminance as significantly higher compared to the GT values for two grayscale patches on the left (black and N3.5), with the TRI054S tendency being considerably higher (see Figure 7c). TRI054S camera accurately measured luminance values for the right three patches (N6.5, N8 and white), suggesting that the overestimation in the left was due to a lens flare effect which had diminished on the right patches. Lastly, Figure 7d shows that both LMK and TRI054S cameras considerably overestimated the luminance of the dark surface area (LMK: 3.77 cd/m^2, TRI054S: 8.71 cd/m^2 and GT: 0.21 cd/m^2), which is again due to a lens flare effect. VIP camera was not able to identify the dark surface due to its small resolution.

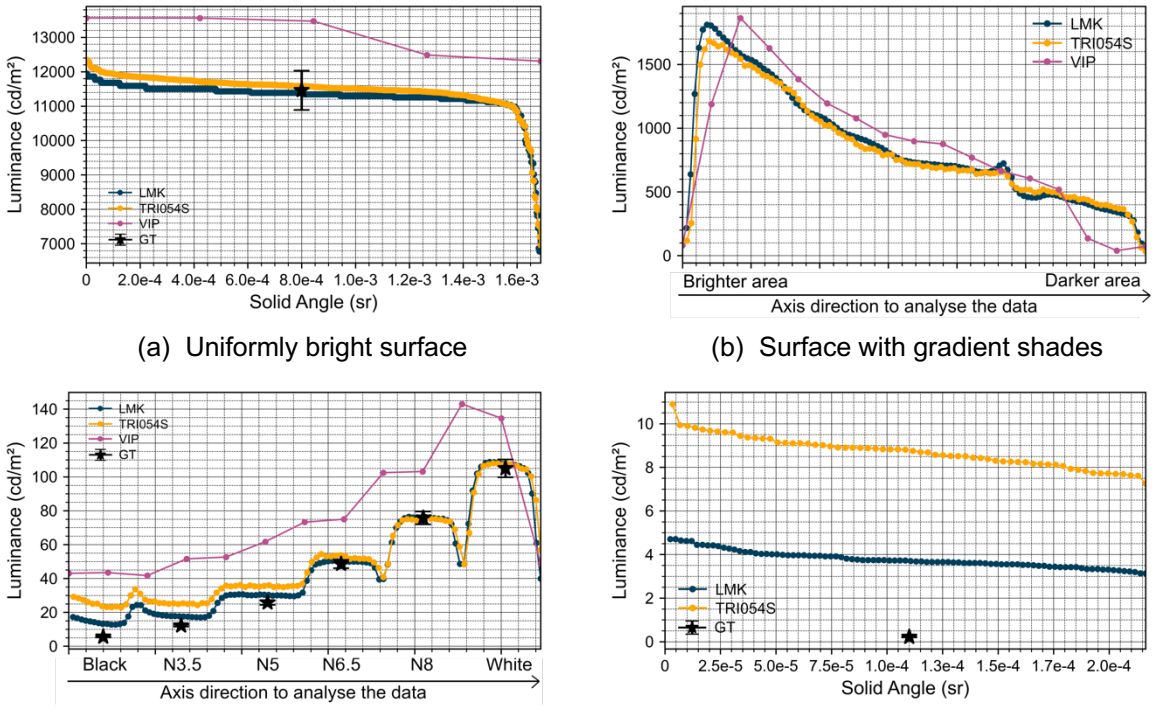

(a) Uniformly bright surface

(b) Surface with gradient shades

(c) Grayscale patches from the color checker

(d) Uniformly dark surface

Figure 7 – Plots of luminance-solidangle showing the comparison results under the Scene C

4 Discussion and Conclusions

In summary, this research introduces a novel experimental framework to assess the luminance measurement performance of different cameras. This framework incorporates a testing environment that replicates common indoor glare conditions and an analytical approach that aligns with real-world indoor glare scenarios. The performance of two state-of-the-art High Dynamic Range (HDR) sensor cameras was then compared within this framework.

The findings indicate that the practical usage of the CSEM VIP camera for glare measurement is approximately two to two-point-five orders of magnitude lower than the range specified (130dB) by Motamed (2017). This is due to the observed negative slope signal characteristic at higher luminance levels. Within its practical usage range (upper limit: 30 kcd/m^2), the camera shows around a 10% error in luminance measurement, assuming a minimum of nine pixels are available for the glare source or the area of interest. When the glare source is small, with fewer than three corresponding pixels, its performance decreased to around a 20% to 25% error. Given the VIP camera's low resolution (320×240 pixels), researchers should be careful when using this camera to measure the luminance of small, non-uniform glare sources or surface areas. However, if above conditions are all satisfied, the VIP camera serves as a reliable tool for daylight glare evaluation. Its compact size makes it especially suited as a wearable glare measurement device, particularly when an ND filter is employed, which can significantly expand its maximum usage range.

The TRI054S camera demonstrates reliable luminance and illuminance measurements, even under high illumination. This camera calculated the illuminance and luminance values of the glare source with a maximum error of 10% in scenarios where an ILMD equipped with a ND3 filter would experience pixel overflow. Furthermore, it measures background luminance (e.g., uniformly bright surface and surface with gradient shades) comparably to an ILMD. However, its performance becomes unreliable (noisy) in lower luminance areas, especially when an intense glare source is within the field of view. In practical terms, if a researcher uses this camera to evaluate discomfort glare when the sun is seen through a roller shade fabric with a 10% openness factor, the camera is likely to accurately measure the luminance and illuminance of only the circumsolar area of the sun disk. Other parts of the image will be fairly noisy.

However, such limitation could potentially be solved by capturing two HDR images, one with an ND filter and one without, and subsequently merging the results. Given the TRI054S camera's ability to capture an HDR image within a minimal exposure time (maximum: 0.15s), such a combination should not produce significant motion artifacts. It should also be noted that this camera is calibrated for evaluating artificial glare sources and background luminance under artificial lighting conditions in this study. When employing this camera in daylight, an appropriate calibration factor (CF) must be derived in advance, as detailed in Section 2.2. Additionally, researcher should be aware of the intrinsic spectral mismatching that can occur with RGB sensors when a photopic V(λ) filter is not used.

In summary, this study shows the potential of HDR sensor cameras in glare evaluation. These devices could offer a higher degree of flexibility compared to conventional devices such as DSLRs or ILMDs with multiple exposure methods. HDR sensor cameras can capture between 7 to 20 HDR images per second, allowing for the real-time monitoring of rapidly changing luminous environments, such as fast-moving clouds or glare sources from a driver's perspective in a vehicle. When used as a head-mounted wearable device, the VIP camera captures glare sources and background luminance based on the users' head movements, providing a more personalized measurement.

Reference

C. Pierson, C. Cauwerts, M. Bodart & J. Wienold. 2021. Tutorial: Luminance Maps for Daylighting Studies from High Dynamic Range Photography. *LEUKOS*, 17:2, 140-169.

A. Krasnoshchoka. 2019. *Diode laser based lighting*. PhD thesis. Technical University of Denmark.

J. Ledig, H. Klinger, C. Schrader. Signal characteristic of a camera with an integrating amplifier and logarithmic encoding at the pixel level. In: *Proceedings of the 29th CIE Session* Washing D.C., USA, June 14 – 22, 2019.

R. Mantiuk, G. Krawczyk, R. Mantiuk & H-P. Seidel. 2007. High Dynamic Range Imaging Pipeline: Perception-motivated Representation of Visual Content. In: *Proc. of Human Vision and Electronic Imaging XII*. 649212

A. Motamed, 2017. *Integrated Daylighting and Artificial Lighting Control based on High Dynamic Range Vision Sensors*. PhD thesis. École Polytechnique Fédérale de Lausanne (EPFL).

S. Lida, Y. *et al.* A 0.68e-RMS random-noise 121dB dynamic-range subpixel architecture CMOS image sensor with LED flicker mitigation. in *IEEE International Electron Devices Meeting (IEDM)*., San Francisco, CA, USA, Dec 1 – 5, 2018, pp. 2–10.

M. Thomas *et al.* 2022. Colour 0.4.2 [Online]. Zenodo. Available from: https://doi.org/10.5281/zenodo.7367239

G. Ward. 1998. hdrgen. [accessed 2023 Jul 14]. http://www.anyhere.com/

G. Ward. 2011. Raw2hdr perl script. [accessed 2023 Jul 14]. http://www.anyhere.com/gward/pickup/raw2hdr.tgz/